$\mathcal{DIFU}_{100}ci@$
Revista de Difusión Científica, Ingeniería y Tecnologías
Vol. 17, No. 2, Mayo - Agosto 2023
ISSN:2007-3585
Artículo arbitrado
Publicado: 31 de agosto de 2023

# Directed Self-assembly of Colloidal Particles on a Blue Phase I Interface

## Auto-ensamblaje Dirigido de Partículas Coloidales Sobre una Interfase de Fase Azul I

**José A. Martínez-González**[*1] and **Stiven Villada-Gil**[2]

[1] *Facultad de Ciencias, Universidad Autónoma de San Luis Potosí.*
Av. Parque Chapultepec 1570, 78210 San Luis Potosí, S.L.P. México.
jose.adrian.martinez@uaslp.mx
[2] *Facultad de Ciencias y Educación, Politécnico Colombiano Jaime Isaza Cadavid.*
Carrera 48 Avenida Las Vegas No. 7-151, 4932 Medellín, Colombia.

**Abstract**

A mean field continuum free energy model of chiral liquid crystals (LCs) is used to consider the self-assembly of colloids and nanoparticles on the surface of a confined Blue Phase I (BPI) with planar anchoring. It is shown that the crystalline defect structure of the blue phase produces intricate, two-dimensional lattices of particles. There are hexagonal and Kagome structures among such arrangements, with lattice parameters that depend on the type of anchoring of the liquid crystal at the colloidal particle's surface. These parameters can be tuned via the chirality of the material, thereby offering intriguing possibilities for the creation of hierarchical materials based on the directed assembly of particles in fluid media.

***Keywords*—** Directed self-assembly, Liquid Crystals, Landau-de Gennes

**Resumen**

Se emplea un modelo de campo medio de la energía libre de cristales líquidos quirales para estudiar el auto-ensamblaje de coloides y nanopartículas sobre la superficie de un cristal líquido quiral de Fase Azul I confinado con anclaje planar. Se muestra que la estructura cristalina de defectos de la fase azul produce arreglos bidimensionales intrincados de partículas. Hay estructuras hexagonales y tipo Kagome entre tales arreglos, con parámetros de red que dependen del tipo de anclaje de las moléculas del cristal líquido sobre la superficie de las partículas coloidales. Estos parámetros pueden modificarse mediante la quiralidad del material, ofreciendo posibilidades peculiares para el desarrollo de materiales con estructuras jerárquicas basadas en el auto-ensamblaje dirigido de partículas en medios fluidos.

***Palabras clave*—** Auto-ensamblaje dirigido, Cristales Líquidos, Landau-de Gennes

## I. Introduction

There is considerable interest in achieving precise control over the position of nanoparticles or colloids for creation of functional materials. In this regard, liquid crystals (LCs) offer unique opportunities. LCs are state of matter that share properties of liquids and crystals. In these phases the molecules can flow while exhibiting order that can be orientational and/or positional. The average molecular orientation of a LC can be described in terms of a vector called nematic director; however, there can be regions where is not possible to define a preferred molecular orientation and those correspond to the so-called topological defects.

Recent experiments and simulations of confined liquid crystals have shown that nanoparticles exhibit a pronounced tendency to segregate to the core of topological defects, thereby minimizing the free energy of the

[*]Autor de correspondencia

composite system [1, 2, 3, 4, 5, 6, 7, 8, 9, 10]. Such demonstrations suggest that liquid crystals could become a viable platform for hierarchical materials assembly. Liquid crystalline blue phases (BP's) represent a morphology where the local director vector field forms double twist cylinders, organized into cubic periodic structures of disclination lines [11, 12]. The question that we address here is whether blue phases can be used to direct the positioning of nanoparticles, and whether the resulting structures have any features that might be difficult to achieve by other means.

Experimental evidence that nanoparticles enhance the thermal stability of blue phases was obtained by Yoshida et al. [13]. They showed that nanoparticle-stabilized blue phases have a texture similar to that of conventional cubic blue phases. Such an increment of stability could be attributed to the fact that nanoparticles move towards the line defects, where they get trapped. How colloidal nanoparticles can assemble into blue phases in bulk and channels have been studied using a mean field Landau-de Gennes approach. These studies show that nanoparticles might very well either aggregate and form clusters along the disclinations lines [9] or assemble in ordered structures [10, 14]. However, to the best of our knowledge, there are not experimental studies about what structures actually emerge. Another concern that arises from past computational studies of colloidal particles in blue phases is the extent to which particles can in fact be solubilized, in the laboratory, in the corresponding liquid crystal. Additionally, the role of the kind of the nanoparticles anchoring in the nanoparticles self-assembly has not been fully addressed. For instance, past studies focused on nanoparticles with homeotropic anchoring and, by considering the intricate behavior of the director field of blue phases, nanoparticles with planar anchoring may respond in a different way; the stable or metastable positions of hometropic particles may not be the same for the planar ones.

Building on the idea that blue phases can be used to template particle assembly, and based on recent experiments showing that particles segregate to the aqueous-liquid crystal interface, in this work we consider the assembly of nanoparticles at the BPI interface. To this end, we rely on a continuum representation of the material, which in a recent study has been shown to provide quantitative agreement with experiment [15]. In a departure from past work, the BPI is confined into a channel whose thickness is sufficiently large as to avoid breaking of symmetry by confinement. We consider nanoparticles with homeotropic and planar anchoring and, in accordance with experiments [16, 17], the BPI is oriented with the (110) plane parallel to the interface.

## II. Methods

The liquid crystals considered here were described in terms of a continuum mean field Landau-de Gennes (LdG) free energy model, which is a fundamental and widely-used theoretical framework in the study of LCs and is particularly powerful in describing their phase transitions and it provides also a quantitative framework for understanding how these materials respond to external perturbations. It considers the LCs system as a continuous and spatially diverse field of order parameters. This order parameter represents the local alignment of the liquid crystal molecules.

In LdG theory the direction of a given molecule and the local average molecular orientation are represented as **a** and **n**, respectively. The scalar order parameter is defined as $S = \left\langle \frac{3}{2}\cos^2\theta - \frac{1}{2} \right\rangle$, with $\cos\theta = \mathbf{a}\cdot\mathbf{n}$; the brackets $<>$ denote a spatial average. The tensor order parameter, $\mathbf{Q}$, is defined by $Q_{ij} = S(n_i n_j - \frac{1}{3}\delta_{ij})$ and is used to express the total free energy $F_{\text{total}}$ as

$$F_{\text{total}} = \int_{\text{bulk}} (F_{\text{phase}} + F_{\text{el}})\,\mathrm{d}V + \int_{\text{surf}} F_{\text{ChannSurf}}\,\mathrm{d}S + \int_{\text{NpSurf}} F_{\text{surf}}\,\mathrm{d}S. \tag{1}$$

$F_{\text{phase}}$ accounts for the short-range interactions, it is given by

$$F_{\text{phase}} = \frac{A}{2}\left(1 - \frac{U}{3}\right) Q_{ij}Q_{ji} + \frac{AU}{3}Q_{ij}Q_{jk}Q_{ki} + \frac{AU}{4}(Q_{ij}Q_{ji})^2, \tag{2}$$

where $A$ is a constant and $U$ is a dimensionless parameter related to the reduced temperature by $\tau = 9(3-U)/U$. In Equation (1), $F_{\text{el}}$ represents the long-range elastic free energy,

$$F_{\text{el}} = \frac{L}{2}\frac{\partial Q_{ij}}{\partial x_k}\frac{\partial Q_{ij}}{\partial x_k} + 2q_0 L\epsilon_{ikl}Q_{ij}\frac{\partial Q_{lj}}{\partial x_k}, \tag{3}$$

where $L$ is the elastic constant, and $q_0 = \frac{2\pi}{p_0}$ is the inverse of the pitch that measures the chirality of the system (and vanishes for non-chiral systems). Here $\epsilon_{ikl}$ is the Levi-Civita tensor. The channel surface free energy $F_{\text{ChannSurf}}$ is given by a Fournier-Galatola [18] expression of the form

$$F_{\text{ChannSurf}} = W\left(\tilde{Q}_{ij} - \tilde{Q}^{\perp}_{ij}\right)^2 \tag{4}$$

where $W$ is the degenerate planar anchoring strength. The $Q$ tensor satisfies $\tilde{Q}_{ij} = Q_{ij} + \frac{1}{3}S_{eq}\delta_{ij}$, with $S_{eq} =$

$\frac{1}{4}\left(1+3\sqrt{1-\frac{8}{3U}}\right)$. Note that $\tilde{Q}_{ij}^{\perp}$ denotes the projection of $\tilde{Q}_{ij}$ on the surface, defined with surface normal $\nu_i$ as $\tilde{Q}_{ij}^{\perp} = P_{ik}\tilde{Q}_{kl}P_{lj}$, where $P_{ij} = \delta_{ij} - \nu_i\nu_j$ is the projection operator. A similar expression, gives the surface free energy for PNp's, while for HNp, it takes the form:

$$F_{\mathrm{NpSurf}} = \frac{1}{2}W_{Np}\left(Q_{ij} - Q_{ij}^{0}\right)^2 \tag{5}$$

where $W_{Np}$ is the nanoparticle anchoring strength and $Q_{ij}^{0}$ is the surface-preferred tensorial order parameter [19].

The following values, which are well in the range expected for common chiral liquid crystals, were used for all calculations: $L = 2.5 \times 10^{-11}$ N, $A = 1.02 \times 10^{5}$ J/m$^3$ [11, 19, 20]. A lattice array with mesh size of 10 nm was used to perform all simulations. The minimization of the free energy was achieved by means of the Euler-Lagrange equation with appropriate boundary conditions [19, 20, 21, 22, 23].

## III. Results and Discussion

### III.1. Structure of the BPI within a planar channel

We present results of simulations for a BPI with chiral pitch, $p = 700$ nm confined into a channel of thickness, $H = 2.1\mu$m. The anchoring at the walls is planar degenerate anchoring with energy $W = 1.2 \times 10^{-3}$ J/m$^2$ . Figure 1a shows a representative structure of the confined BPI. In this and subsequent figures, the color indicates the orientation of the local director: it is blue when the molecules are parallel to planar surfaces ($x-y$ plane), and red when they are perpendicular to such surfaces (or parallel to the $z$ axis). We find that strong planar anchoring at each interface distorts the disclination lines mainly along the first 300 nm, and a well-formed BPI is obtained in the central region of the system (see Fig. 1b). Having shown that the BPI can be confined under these conditions, we can now proceed to examine the interfaces of the system which, by symmetry, have the same properties, thereby allowing us to focus on one of them. Figure 2 shows the upper section of the system, where one can clearly see the director field at the interface. Although somehow distorted, the $\lambda^{-\frac{1}{2}}$ disclination lines reach the interface. As a consequence, the director field on the surfaces has a pattern of $\lambda^{-\frac{1}{2}}$, as well as $\lambda^{+1}$ defects with the symmetry of the (110) plane of the BPI in bulk (Fig. 2), and a global topological charge of zero. Moreover, the $\lambda^{+1}$ defects form an hexagonal array with lattice parameters $a_1 = p$ and $a_2 = \sqrt{3}p/2$.

The BPI is oriented with the (110) plane parallel to the interface, and this makes a remarkable difference with respect to previous studies of BPI confined into channels [24, 25]. If such an orientation is not taken into account,

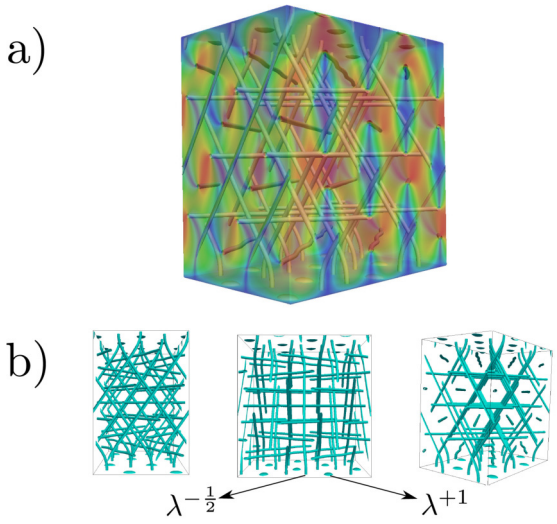


**Figure 1:** *a) A confined BPI into a channel with planar anchoring. The color represents the orientation of the local director. The figure was made slightly transparent to allow the disclination lines to be seen. b) Different lateral views of the disclination lines show how the line defects bend at the proximity of the interface.*

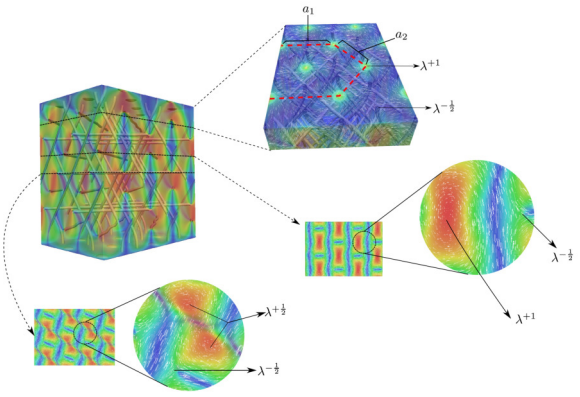


**Figure 2:** *Upper and transversal sections of the confined BPI. The hexagonal array of the $\lambda^{+1}$ defects at the interface has lattice parameter $a_1 = p$ and $a_2 = \sqrt{3}p/2$. All the transversal sections have zero topological charge.*

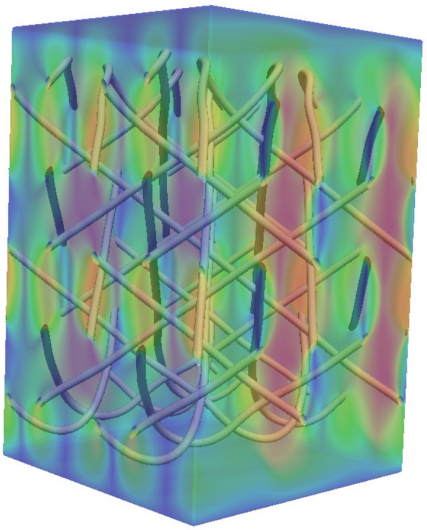

**Figure 3:** *Disclination lines in a BPI with the (100) plane parallel to the interface. This structure has higher free energy than the case with the (110) plane parallel to the channel's surface.*

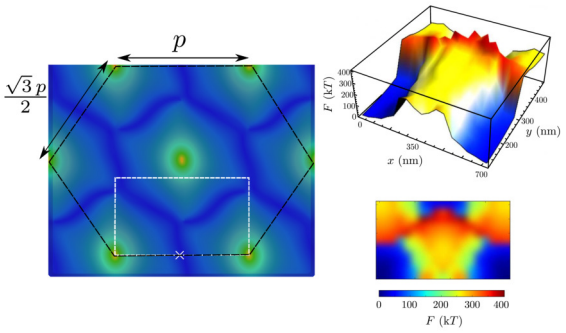


**Figure 4:** *(Left) Section of the top surface of the system. A HNp was deposited on different positions of the selected region to obtain the spatial dependence of the free energy (right). The free energy when the HNp is located on the $\lambda^{+1}$ site was taken as reference. The corresponding metastable position is marked by the X in the left figure.*

the planar anchoring at the interface intensifies the strain on the BPI-unit cells and increases the free energy. As a consequence, in the case of a BPI with the (100) planes parallel to the interface [24, 25], the disclination lines do not reach the interface (Fig.3).

### III.2. Nanoparticles deposition

For nanoparticle assembly, we consider particles with radius, $R = 120$ nm with planar and homeotropic anchoring with $W_{\rm P} = W_{\rm H} = 2.5 \times 10^{-4}$ J/m$^2$. First, we determine the positions on the surface which are most energetically favorable for deposition of nanoparticles having planar and homeotropic anchoring, respectively. Next, we proceed to analyze 50-50% mixtures of homeotropic (HNp) and planar (PNp) nanoparticles and, lastly, we consider the particular case of a mixture of 75% HNp and 25% PNp.

Figure 4 shows a free energy map for a HNp. We can appreciate from the figure that the sites with lower free energy correspond to the positions of the $\lambda^{+1}$ point defects, which were taken as reference. Interestingly, there are also metastable states which do not correspond to the positions of $\lambda^{-\frac{1}{2}}$ defects but a location between them. Such regions also adopt a hexagonal arrangement, with the same lattice parameters than those obtained for the $\lambda^{+1}$ defects. This implies that only half of the sites between the $\lambda^{-\frac{1}{2}}$ defects are metastable. A closer look at a HNp on a metastable site shows that the disclination lines approach the bottom of the particle. This changes the symmetry of the system at the interface (Fig. 5). Based on these observations, we predict that HNp's deposited on a BPI interface with planar anchoring will primarily assemble following the $\lambda^{+1}$-hexagonal array with lattice parameters $a_1 = p$ and $a_2 = \sqrt{3}p/2$, but that metastable positions will also be filled without giving rise to "crystallographic defects".

Parallel particles (PNp's) only exhibit free energy minima at the $\lambda^{+1}$ positions. For this case, the sites between $\lambda^{-\frac{1}{2}}$ defects correspond to saddle points in the free energy landscape (Fig. 6). This finding suggests a possible pathway to study particle assembly in HNp-PNp mixtures or, more precisely, the deposition of PNp's followed by HNp's. To do so, we first simulate a 50-50 mixture of HNp and PNp. First, eight PNp's are positioned on the $\lambda^{+1}$ sites, followed by eight HNp's placed in what were their metastable positions (Fig. 7a). For such a nanoparticle distribution, there is enough room to place additional nanoparticles that could give rise to more compact structures. In the HNp-free energy surface (Fig. 4), it is possible to identify regions that, once the preferred sites are occupied, could be populated without a large energetic cost. By taking into account the nanoparticle's size, such regions correspond to the available sites between $\lambda^{-\frac{1}{2}}$ defects. The resulting compact structure represents a Kagome-like array (Fig. 7b). We estimate that the free energy difference between the hexagonal and Kagome structures is 296 $k_BT$, with the hexagonal array being more stable. The Kagome lattice, however, can become more favorable at higher concentrations. We also studied a system comprising eight PNp's and twenty-four HNp's, which results in an hexagonal array of PNp's and a Kagome structure for HNp's (Fig. 8).

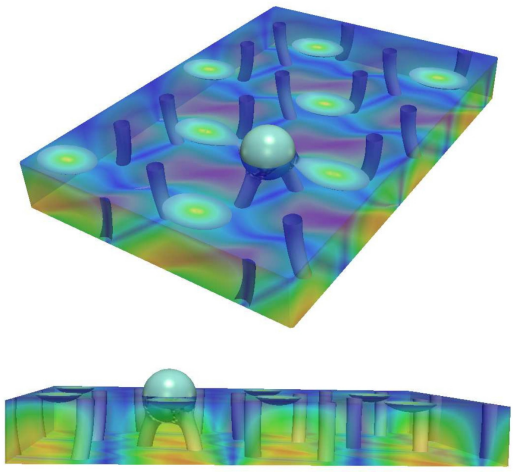

**Figure 5:** *Top and lateral view of the disclination lines when a HNp is placed at a metastable site. Such a site is located between two $\lambda^{-\frac{1}{2}}$, the disclination lines now bend toward the particle bottom as they approach at the interface.*

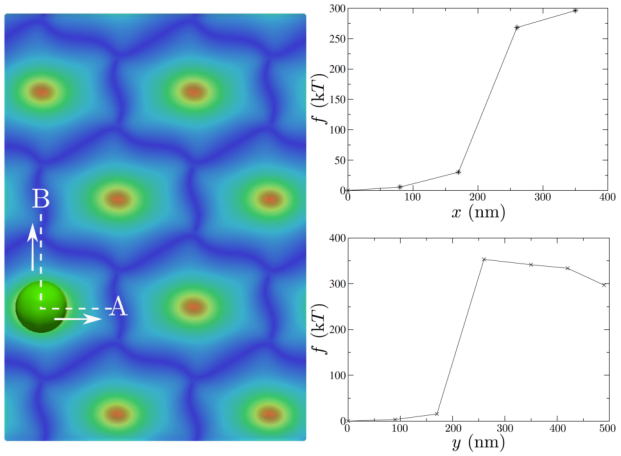


**Figure 6:** *Free energy as a function of the distance for a PNp that is moving from its minimum energy position, which is taken as a reference, in the $x$ and $y$ directions respectively. Note that A and B positions are equivalent.*

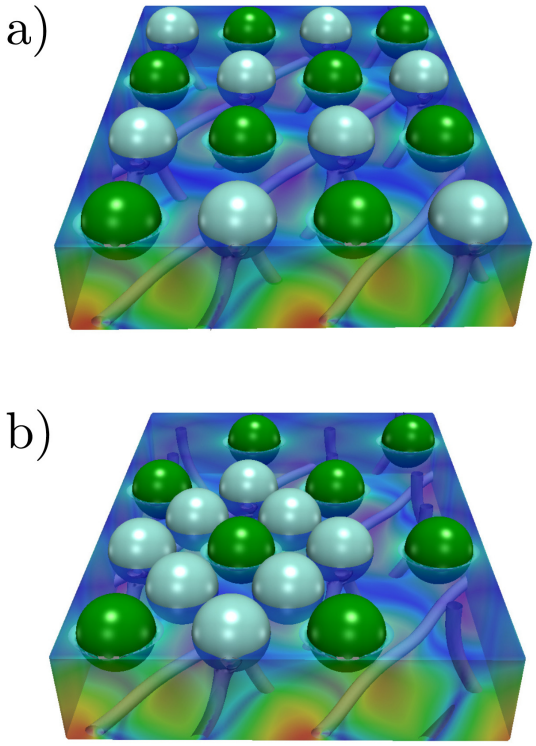


**Figure 7:** *a) A 50-50 mixture of PNp's (green) and HNp's (blue). The PNp's are placed on the $\lambda^{+1}$ defects while the HNp's fill out what were their metastable positions. Both kind of nanoparticles form an hexagonal array of the same size. b) The same number of nanoparticles but in a more compact Kagome-like structure.*

Experimentally, these colloidal crystalline structures formed by particles with different anchoring can be obtained by taking advantage of either nano-particle sputter-doping method [13] or a combination of forming particles in-situ [26] and nano-particle sputter-doping technique. Following Yoshida et al., one could use sputter-doping to fabricate a highly dispersed nanoparticle-liquid crystal suspension with target particles [13]. Alternatively, the second colloidal particles could be generated through the phase separation of chiral liquid crystal from the second component in a binary mixture by quenching the blue phase. Since all the lattice parameters of the structures so far depend on the pitch, the BPI-channel offers a possibility of having a crystalline colloidal assembly that can be tuned via chirality and particle concentration.

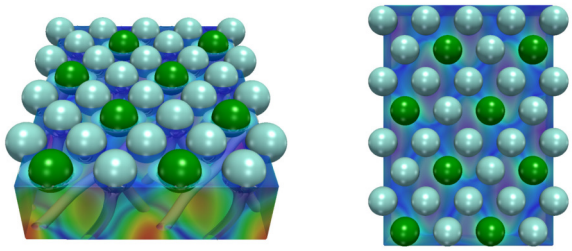

**Figure 8:** *A 25-75% mixture of PNp and HNp respectively, where the PNp's form an hexagonal array while the HNp's assemble in a Kagome structure.*

## IV. Conclusions

At the BPI-planar interface, colloids prefer to localize in the regions with the highest free energy, which correspond to the cores of $\lambda^{-1/2}$-topological defects followed by the $\lambda^{+1}$ defects. Therefore, a hexagonal array of colloidal particles can be produced, with a lattice parameter that depends on the chiral pitch (Fig. 4). Interestingly, for planar nanoparticles, only the regions with $\lambda^{-1/2}$-topological defects are the preferred while homeotropic nanoparticles can also localized at regions with $\lambda^{+1}$ defects. This fact enables the possibility of directing the self-assembly of colloids to form different crystalline arrangements. Particularly, a gradual deposition of colloids according to their surface anchoring can induce the formation of hexagonal and kagome lattices. This study shows how ordered structures of particles can be achieved on a fluid media, where the morphology of the lattices can be tuned via chirality and be destroyed and reproduced in terms of the phase behavior of the liquid crystal.

## Acknowledgments

We acknowledge support from Ciencia de Frontera CONACYT grant CF-2019-74885.

## References

[1] Marcello Cavallaro Jr et al. «Exploiting imperfections in the bulk to direct assembly of surface colloids». In: *Proceedings of the National Academy of Sciences* 110.47 (2013), pp. 18804–18808.

[2] Mohammad Rahimi et al. «Nanoparticle self-assembly at the interface of liquid crystal droplets». In: *Proceedings of the National Academy of Sciences* 112.17 (2015), pp. 5297–5302.

[3] Miha Škarabot et al. «Hierarchical self-assembly of nematic colloidal superstructures». In: *Physical Review E* 77.6 (2008), p. 061706.

[4] David Pires, Jean-Baptiste Fleury, and Yves Galerne. «Colloid particles in the interaction field of a disclination line in a nematic phase». In: *Physical Review Letters* 98.24 (2007), p. 247801.

[5] Jonathan K Whitmer et al. «Nematic-field-driven positioning of particles in liquid crystal droplets». In: *Physical review letters* 111.22 (2013), p. 227801.

[6] Jun-ichi Fukuda et al. «Stability of cholesteric blue phases in the presence of a guest component». In: *Physical Review E* 86.4 (2012), p. 041704.

[7] Brigita Rožič et al. «Theoretical and experimental study of the nanoparticle-driven blue phase stabilisation». In: *The European Physical Journal E* 34.2 (2011), p. 17.

[8] Emine Kemiklioglu, Jeoung-Yeon Hwang, and Liang-Chy Chien. «Stabilization of cholesteric blue phases using polymerized nanoparticles». In: *Physical Review E* 89.4 (2014), p. 042502.

[9] Kevin Stratford et al. «Self-assembly of colloid-cholesteric composites provides a possible route to switchable optical materials». In: *Nature communications* 5.1 (2014), p. 3954.

[10] Miha Ravnik et al. «Three-dimensional colloidal crystals in liquid crystalline blue phases». In: *Proceedings of the National Academy of Sciences* 108.13 (2011), pp. 5188–5192.

[11] David C Wright and N David Mermin. «Crystalline liquids: the blue phases». In: *Reviews of Modern physics* 61.2 (1989), p. 385.

[12] PP Crooker. «The cholesteric blue phase: A progress report». In: *Molecular Crystals and Liquid Crystals* 98.1 (1983), pp. 31–45.

[13] Hiroyuki Yoshida et al. «Nanoparticle-stabilized cholesteric blue phases». In: *Applied physics express* 2.12 (2009), p. 121501.

[14] Miha Ravnik et al. «Confining blue phase colloids to thin layers». In: *Soft Matter* 7.21 (2011), pp. 10144–10150.

[15] José A Martínez-González et al. «Blue-phase liquid crystal droplets». In: *Proceedings of the National Academy of Sciences* 112.43 (2015), pp. 13195–13200.

[16] Jin Yan et al. «Angular dependent reflections of a monodomain blue phase liquid crystal». In: *Journal of Applied Physics* 114.11 (2013).

[17] Tsung-Hsien Lin et al. «Red, green and blue reflections enabled in an optically tunable self-organized 3D cubic nanostructured thin film». In: *Advanced Materials* 25.36 (2013), pp. 5050–5054.

[18] J-B Fournier and Paolo Galatola. «Modeling planar degenerate wetting and anchoring in nematic liquid crystals». In: *Europhysics Letters* 72.3 (2005), p. 403.

[19] Miha Ravnik et al. «Mesoscopic modelling of colloids in chiral nematics». In: *Faraday discussions* 144 (2010), pp. 159–169.

[20] A Dupuis, D Marenduzzo, and JM Yeomans. «Numerical calculations of the phase diagram of cubic blue phases in cholesteric liquid crystals». In: *Physical Review E* 71.1 (2005), p. 011703.

[21] GP Alexander and JM Yeomans. «Numerical results for the blue phases». In: *Liquid Crystals* 36.10-11 (2009), pp. 1215–1227.

[22] Miha Ravnik and Slobodan Žumer. «Landau–de Gennes modelling of nematic liquid crystal colloids». In: *Liquid Crystals* 36.10-11 (2009), pp. 1201–1214.

[23] V Tomar et al. «Morphological transitions in liquid crystal nanodroplets». In: *Soft Matter* 8.33 (2012), pp. 8679–8689.

[24] Jun-ichi Fukuda, Slobodan Žumer, et al. «Novel defect structures in a strongly confined liquid-crystalline blue phase». In: *Physical review letters* 104.1 (2010), p. 017801.

[25] Jun-ichi Fukuda, Slobodan Žumer, et al. «Field-induced dynamics and structures in a cholesteric-blue-phase cell». In: *Physical Review E* 87.4 (2013), p. 042506.

[26] Jean-Christophe Loudet, Philippe Barois, and Philippe Poulin. «Colloidal ordering from phase separation in a liquid-crystalline continuous phase». In: *Nature* 407.6804 (2000), pp. 611–613.